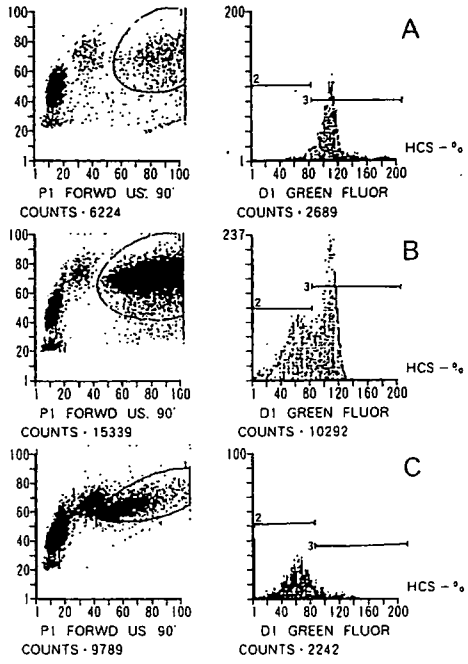

図9　骨髄球系細胞[MXGA(+)CD 16(−)]を対象にMY 4 抗体を用いての single color での解析．A：重症RA 患者脛骨の骨髄球分画，B：重症 RA 患者腸骨の骨髄球分画，C：健常人対照の腸骨の正常の骨髄球．

腸骨骨髄中の細胞の変化は関節破壊の広がりの自然経過によって異なった特徴を示した(図 10)．骨髄細胞病態だけで言うならば，HLA-DR(+)CD 8(+)の T cell の増加が見られる状態が多発性の滑膜増殖を伴う RA の一般型(LES)であり，ここに異常な骨髄球系細胞の誘発が加われば MES になるのではないか．異常な骨髄球系の反応は靱帯や骨の高度の変性変化を導くもので，MUD の病像はその典型ではないか．MES では異常な骨髄球系の分化が，活性化された T 細胞によってむしろ抑えられて[12]，MUD ほどの極端な組織破壊を示さないのではないか．また視点を変えれば，RA の病型あるいは予後診断の手がかりは，腸骨の単核細胞分画を調べることによっても可能である(表 1)と考えられた．骨髄の細胞の病態の詳細については本稿では割愛させていただく．

III. 治療方針

RA に対する基本的な治療[13]は，精神的なことも含めての日常生活上の配慮と薬物療法であることは言うまでもない．RA であれば抗リウマチ剤(DMARDs)という考えを改めるべきと考えている．たとえば，骨髄病態のみで考察してみよう．図 7 に示したように

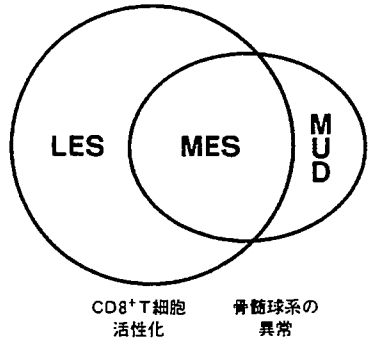

図 10　腸骨骨髄単核球分画の変化と RA 病型．

CD 8(+)T 細胞の活性化が LES と MES に特徴的病態であり，異常な(癌特異抗原をもった)骨髄球系細胞の分化が MES と MUD で特徴的である．単純に考えても，LES には DMARD を，MES には DMARD と免疫抑制剤の併用を，MUD には強力な免疫抑制剤をというのが妥当ではないか．われわれは基本的にはそのような投与方針を続けてよい感触を得ている．

もう 1 つ大切なことは LES の患者の場合には，自然経過として重度の身体障害に陥りにくいので無理な治療をするべきでないことである．すなわち，副作用いかんでは DMARD などの投薬をやめて日常の節制に注意を促すほうがよい治療と言える場合もある．精神的な安寧と充分な睡眠で寛解期を続けうることは臨床的によく経験されることである．さらに，長期の寛解期に入った患者に DMARD の投与をどの段階でやめるかも問題である．筆者自身は CRP が正常域になって 1 年以上の患者には DMARD を止めて経過を観察している．

基本的なことは以上のようなものであるが，われわれは整形外科医なので，以下の稿は整形外科的な治療法に関して述べる．従来，整形外科医が RA 治療に深く関与してきたのは滑膜切除術と人工関節手術を通してであることより，この両手術と日常診療で多い中足部変形について述べる．

A．滑膜切除術

従来，整形外科医が RA 治療に深く関与してきたのは滑膜切除術を通してであった．滑膜切除術は RA による骨破壊を抑えると言われてきた．われわれは，滑膜切除術は骨破壊の進行は抑ええず病型の自然経過のままである[10]が，関節局所の腫脹疼痛を抑えて臨床的には有用なよい手術と考えている．

1．一般的な概念

滑膜切除手術は特に LES の患者には優れた臨床効果

表2　手関節の早期滑膜切除術後の臨床症状(右半分)とX線写真(左半分)の評価

Subset	Followup (yr)	Satisfactory Ratings: Radiographic Ope (%)	Nonope (%)	χ^2	p Value	Clinical Ope (%)	Nonope (%)	χ^2	p Value
LES	1	81(22)	74(20)	0.57	>0.05	93(25)	44(12)	4.22	<0.001
(N=27)	5	48(13)	40(11)	0.55	>0.05	81(22)	74(20)	0.65	>0.05
MES	1	0(0)	0(0)	0	>0.05	87(13)	40(6)	2.66	<0.01
(N=15)	5	0(0)	0(0)	0	>0.05	60(9)	53(8)	0.37	>0.05
MUD	1	0(0)	0(0)	0	>0.05	0(0)	0(0)	0	>0.05
(N=5)	5	0(0)	0(0)	0	>0.05	0(0)	0(0)	0	>0.05

臨床症状は腫脹，疼痛の改善例を，X線写真では進行の認められない例を成績良好(satisfactory)として術後1年と5年で評価した．

を示す．MESの患者の早期には価値ある手術と思うが，MUDの患者では通常は滑膜の増殖は乏しく滑膜切除は無意味である．滑膜切除術の効用に関して次のように考えている．

①特定の関節腫脹と疼痛が強いために鎮痛消炎剤や抗リウマチ剤の増量が6カ月以上続いている例にはぜひ行うべき手術である．

以下に述べるが，RA関節の疼痛や腫脹などの臨床症状に対する滑膜切除術の効果は(特にLESに対しては)優れている．滑膜切除術によって疼痛が減り，鎮痛消炎剤の全身投与量を抑えることができれば，全身的にはすばらしい効果と考えている．

②活動性の病巣を減らして抗リウマチ剤を効きやすくする．

抗リウマチ剤がRAを抑えうるとすれば，罹病早期のまだ病巣があまり広がっていない段階であろう．さらに病巣を少なくしようと考えれば，(複数関節でも)滑膜切除は有力な一手段である．その状態で抗リウマチ剤を用いれば優れた効果が得られると考えている．吉野ら[18]の主張する多関節の滑膜切除術は早期に行い，適切な薬物治療と組み合わせることによって優れた臨床効果をあげうると思う．

2．手関節の滑膜切除術の効果[13]

代表的な滑膜切除術として手関節に対する手術の効果を述べる．

a．臨床症状に対する効果

表2右半分は手関節の早期滑膜切除術後の臨床症状として腫脹，疼痛ともに改善した例を術後1年と5年で評価したものである．術後1年では少関節破壊型(LES)(p<0.001)，多関節破壊型(MES)(p<0.01)とも明らかに有効である．5年では，特にLESでは長期寛解に向かう例も多いために非手術側との間に有意差は認められなくなる(p>0.05)．MUDでは通常は滑膜増殖はごく限られた部分に認められる程度で，滑膜切除術はあまり意味がないと感じながら手術をしたが，やはり短期成績でも有意な臨床成績の改善を認めなかった(p>0.05)．

b．骨破壊の進行に対する効果

滑膜切除術の効果を，まず手術前後の単純X線写真をSteinbrockerらのStage分類[17]で評価し，観察開始時に比し進行のないものを評価した(表2左半分)．手術群と非手術群の間に統計的有意差を認めなかった(p>0.05)．そこで，もっと詳細な評価方法で骨破壊の進行を評価して，滑膜切除術が手関節破壊の進行の速度を緩めないかを検討した．手根骨の破壊の速さはYoumら[19]の提唱するcalpal height ratio (CHR)(図6)の一定期間での減少を測定することにより詳細な評価が可能と考えたからである．方法は片側手関節の早期滑膜切除術を行った患者(LES 27例，MES 15例，MUD 5例)を対象に手術手の手根骨の破壊の速さが非手術手よりも抑えられたかを検討した．RAにより中手骨はほとんど破壊されないことより，手根骨の破壊の速さは経時的にCHRを測定し，その1年当りの減少(△CHR[17])で評価した．表3に示されるように△CHRでの評価によっても手術手が非手術手より改善されている傾向は認められなかった(p>0.05)．ただ各病型間では高度の(p<0.001)有意差を示し，滑膜切除手術をしても骨破壊に関しては自然経過のままという面が明確に示された．

B．人工関節手術の適応

RA患者に対する人工関節手術は各関節に適応となるが，最も必要性の高いものの1つである人工膝関節を

表3 滑膜切除術の手根骨の破壊の速さに対する効果

病 型	非手術手	手術手	p値
LES (N=27)	0.006(0.005)	0.005(0.004)	>0.05
MES (N=15)	0.025(0.009)	0.029(0.013)	>0.05
MED (N=5)	0.095(0.046)	0.099(0.044)	>0.05

CHRの1年当りの減少(△CHR[9])で評価した.

表4 X線的変化のある膝関節破壊の進行と炎症反応値の関連

MES(N=35)	CRP(mg/dl)	RF(IU/ml)
1年以上狭少化のまま (N=25)	2.2(0.6-3.9)	141(24-275)
1年以内に人工関節 (N=10)	7.0(4.3-8.3)	117(66-207)
MUD(N=11)		
1年以内に人工関節 (N=11)	8.8(7.0-12.0)	234(58-380)

例にとって述べる.

大阪大学附属病院で行われた成人(60歳以下)発症RAに対する人工関節手術例の1987年の集計を,あとから病型と術前の経過別に分類して検討した.46膝関節(31症例,男性6例,女性25例)のうちLESの症例はなく,MESの症例は35関節(24症例,男性5例,女性19例),MUDの症例は11関節(7症例,男性1例,女性6例)であった.成人発症RAでLESと考えられるときにはX線で認められるほどの膝関節破壊に陥ることは少ない.その結果とも言えるが,将来膝の人工関節手術が必要になる可能性はきわめて少ないと言える.

人工膝関節手術を行ったこれら46膝の手術前数年間のX線所見を観察した(表4).MESの35例のうち関節裂隙の狭小化の状態で1年以上歩行能力が維持できた25例では,CRP値は0.6-3.9 mg/dlで平均2.2 mg/dlを示した.一方,骨破壊が急速に進み1年以内に歩行不可となり人工関節手術を必要とした10例では,CRP値は4.3-8.3 mg/dlで平均7.0 mg/dlであった.MUDの11例では全例関節破壊が急速に進み,歩行能力を失い人工関節手術を必要としたが,CRP値は7.0-12.0 mg/dlで平均8.8 mg/dlを示した.

MESの場合には人工関節手術に至るとしても,薬物療法などで炎症状態を4 mg/dl以下に抑えることができれば補助装具の使用などにより手術の時期を延ばしうることが示された.MUDの場合には薬剤などで炎症反応を抑えることは事実上きわめて困難と思われた.

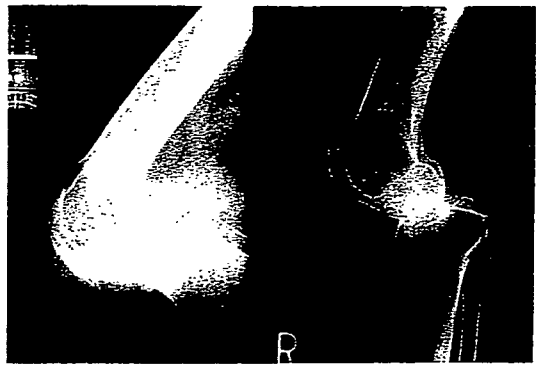

図11 MUD症例の膝関節の側面運動像.左は屈曲位,右は伸展位.脛骨関節面前縁と大腿骨顆部後縁が接しての屈伸である.

骨が非常に脆くなっているMUDの患者では手術時期には特に注意するべきである.図11はMUD症例の膝関節の側面運動像である.靱帯などの膝関節支持機構が弛み,脛骨関節面が大腿骨顆部に対して亜脱臼を起こした状態で屈伸している.脛骨関節面前縁と大腿骨顆部後縁が接しての屈伸である.負荷が続くと,骨が脆弱なために接面からの圧壊が進むのが大きな骨破壊機序である.上下肢各関節において基本的にはこのような現象が起きてくるのがMUDの特徴である.そのような機序によりどんどん破壊が続くので,手術時期を遅らせると関節部の骨構築が崩れて,望ましい形での人工関節置換が困難となる.MUDの患者の場合には明らかに関節機能が失われれば,できるだけ早急に人工関節手術を行い機能を保持させることが大切である.このことは下肢のみでなく上肢の人工関節手術にも言える.

C. 中足部破壊の問題

中足部の関節破壊のために,特にでこぼこ道では痛くて歩けない症例は多い.中足部の破壊[2]は距舟関節の狭小化で留まるか骨性強直してしまう例が多い.しかし症例により,距骨頭が底側に亜脱臼して縦軸アーチが崩れるとともに踵骨の外反が進み,典型的な外反偏平足に陥っていく例をしばしば見受ける.

中足部変形の経過も病型によって異なる.足の縦軸アーチの底部長に対するアーチの高さの比でアーチの破壊を評価した(横倉法).この比の経年的な進行が図12に示されている.図12左に示されるLESではアーチの崩れは見られない.しかし,MESとMUDを示す

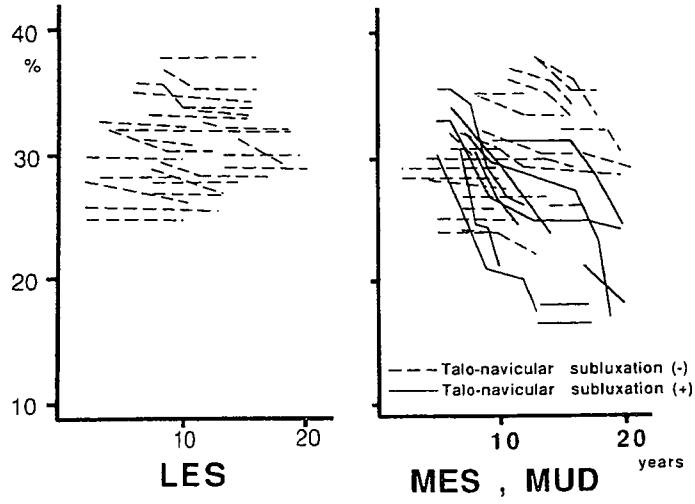

図 12　RA 中足部縦軸アーチ破壊の進行評価：足の縦軸アーチの底部長に対するアーチの高さの比(横倉法)を指標にして縦軸にとり，罹病年数を横軸にとったもの.

図 12 右ではアーチが崩れる症例が認められ，特に MUD では全例がそうである．われわれは RA 患者の中足部破壊に対して，LES 症例には足底挿板使用で観察している．MES 症例には足底挿板を使用しながら観察して，距骨頭の底側亜脱臼が始まれば距舟関節固定術を施行している．MUD 症例の場合には，中足部破壊が始まれば急速に崩れていくので 3 関節固定を施行している.

V. ま と め

以上の論旨をまとめると以下のようになる．すなわち，① RA 患者は自然経過として 3 病型に分けられ予後診断は可能である．②全身性の(腸骨)骨髄細胞の病態も 3 病型で異なる．③薬物療法も手術療法も病型別に検討するべきではないか(図 13).

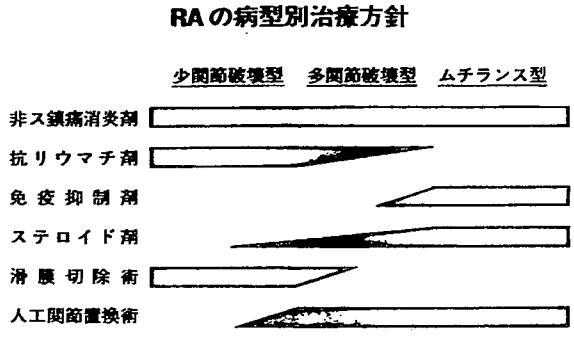

図 13　RA 病型別の治療方針.

文　献

1) Arnett, F.C., et al.: The American Rheumatism Association 1987 revised criteria for the classification of rheumatoid arthritis. Arthritis Rheum.,**31**：315-324, 1988.
2) 東文造他：慢性関節リウマチの後足部変形の自然経過とその手術療法．臨床リウマチ，**4**：121-127, 1991.
3) Fujimoto, M., et al.: Fluctuation of interleukin-1 and -6 activity in bone marrow serum in collagen-induced arthritis in rats. Biomedical Res., **13**：243-251, 1992.
4) Fujimoto, M., et al.: Elevated activity of interleukin-1, -2, and -3 in the bone marrow of collagen-induced rat. Biomedical Research, **9**：401-407, 1988.
5) Hayashida, K., et al.: Bone marrow changes in adjuvant-induced and collagen-induced arthritis. Arthritis Rheum., **35**：241-245, 1992.
6) 西岡久寿樹他：早期リウマチの疫学に関する研究班，平成 3 年度厚生省リウマチ調査研究事業研究報告書，厚生省，1-21, 1993.
7) Ochi, T., et al.: Natural course of joint destruction and fluctuation of serum C1q levels in patients with rheumatoid arthritis. Arthritis Rheum., **31**：37-43, 1988.
8) Ochi, T., et al.: The presence of a myeloid cell population showing strong reactivity with monoclonal antibody directed to difucosyl type 2 chain in epiphyseal bone marrow adjacent to

joints affected with rheumatoid arthritis and its absence in the corresponding normal and non-RA bone marrow. J. Rheumatol., **15**：1609-1615, 1988.
9) 越智隆弘：重症慢性関節リウマチの病態．リウマチ，**30**：287-300, 1990.
10) Ochi, T., et al.: Effect of early synovectomy on the course of rheumatoid arthritis. J. Rheumatol., **18**：1794-1798, 1991.
11) 越智隆弘他：同種胸腺細胞移植によるマウス多発関節炎における発症と増悪の要因．臨床免疫，**23**：1419-1427, 1991.
12) 越智隆弘他：病態解明に関する研究班，平成3年度厚生省リウマチ調査研究事業研究報告書，厚生省，75-165, 1993.
13) 越智隆弘：慢性関節リウマチの治療法．臨床科学，**29**：105-108, 1993.
14) Owaki, H., et al.: Elevated activity of myeloid growth factor in bone marrow adjacent to joints affected by rheumatoid arthritis. J. Rheumatol., **16**：572-577, 1989.
15) Owaki, H., et al.: Facs analysis of myeloid differentiation stages in epiphyseal bone marrow, adjacent to joint affected with rheumatoid arthritis. Scand. J. Rheumatol., **20**：91-97, 1991.
16) 島岡康則他：高齢発症慢性関節リウマチについて．中部整災誌，**33**：869-871, 1990.
17) Steinbrocker, O., Traeger, C.H. and Batterman, R.C.: Therapeutic criteria in rheumatoid arthritis. JAMA, **140**：659-662, 1949.
18) 吉野慎一，小和田誠，小岩政仁：根治的多関節滑膜切除術－新しい関節リウマチの治療戦略として－．日整会誌，**67**：S 487-S488, 1993.(抄)
19) Youm, Y., et al.: Kinematics of the wrist. I.An experimental study of radio-ulnar deviation and flexion-extension. J. Bone Joint Surg., **60-A**：423-431, 1978.

Scand J Rheumatol 20: 91–97, 1991

Facs Analysis of Myeloid Differentiation Stages in Epiphyseal Bone Marrow, Adjacent to Joints Affected with Rheumatoid Arthritis

H. OWAKI[1], K. YUKAWA[2], T. OCHI[1], Y. SHIMAOKA[1] and K. ONO[1]

[1]Department of Orthopaedic Surgery, and [2]Institute for Molecular and Cellular Biology, Osaka University Medical School, Osaka, Japan

Owaki H, Yukawa K, Ochi T, Shimaoka Y and Ono K. Facs Analysis of Myeloid Differentiation Stages in Epiphyseal Bone Marrow, Adjacent to Joints Affected with Rheumatoid Arthritis. Scand J Rheumatol 1990; 20: 91–97.

To analyze the differentiation stages of myeloids statistically, we adopted a two-color FACS system and used appropriate monoclonal antibodies belonging to CD15, CD16 and CD11b. By using HL60 treated with DMSO or human bone marrow MNCs from patients with rheumatoid arthritis, it was proved that with this system, myeloids could be clearly separated according to differentiation stages. Furthermore, the number of myeloids at certain stages of differentiation in the epiphyseal bone marrow of patients with RA or OA was measured. Nine of 15 samples from RA patients showed immature and relatively mature myeloids, while none of the 8 OA samples did. When the proportions of myeloids in epiphyseal bone marrow MNCs were compared with the clinical features, disease subsets in RA and the degree of synovitis, seemed to be important factors for abnormal myelopoiesis.

Key words: rheumatoid arthritis, bone marrow, myeloids

Hajime Owaki, 8650 Southwestern Blvd. #2811, Dallas, Texas 75206, USA

We have previously reported the presence of myeloid lineage cells in the epiphyseal bone marrow, adjacent to joints affected with rheumatoid arthritis, and the absence of these cells in normal or non-RA joints(1). Following this report, we demonstrated a highly active myeloid growth factor in corresponding sites in RA(2) and indicated this could be an important factor for abnormal myelopoiesis. To study this phenomenon in more detail, it is necessary to determine the spectrum of the differentiation stages of these abnormally accumulated myeloids. Some specific cytoplasmic markers for differentiation of myeloids are known, such as lactoferrin(3), but these are not useful for quantitative analysis. On the other hand, Fluorescence Activated Cell Sorter (FACS) analysis, using monoclonal antibodies for the cell surface marker, is a powerful tool for quantitative study, even though the technique is very simple. In this study, we analyzed the differentiation stages of myeloids with FACS. For this purpose, we first used HL60, a well known myeloblastic leukemia cell line, differentiated into myelo-granulocytic lineage cells, in reaction to stimulation with chemical such as dimethyl-sulfoxide (DMSO)(4). We next analyzed the quantities of epiphyseal bone marrow cells in rheumatoid arthritis (RA) and osteoarthritis (OA) cases and compared the results with clinical findings.

MATERIALS AND METHODS

Patients

Fifteen joints from 13 patients diagnosed as RA according to the criteria of the American Rheumatism Association(5) were studied. There were 2 men and 11 women with an age range of 30–71 (mean 52). According to our classification of disease severity for RA(6),

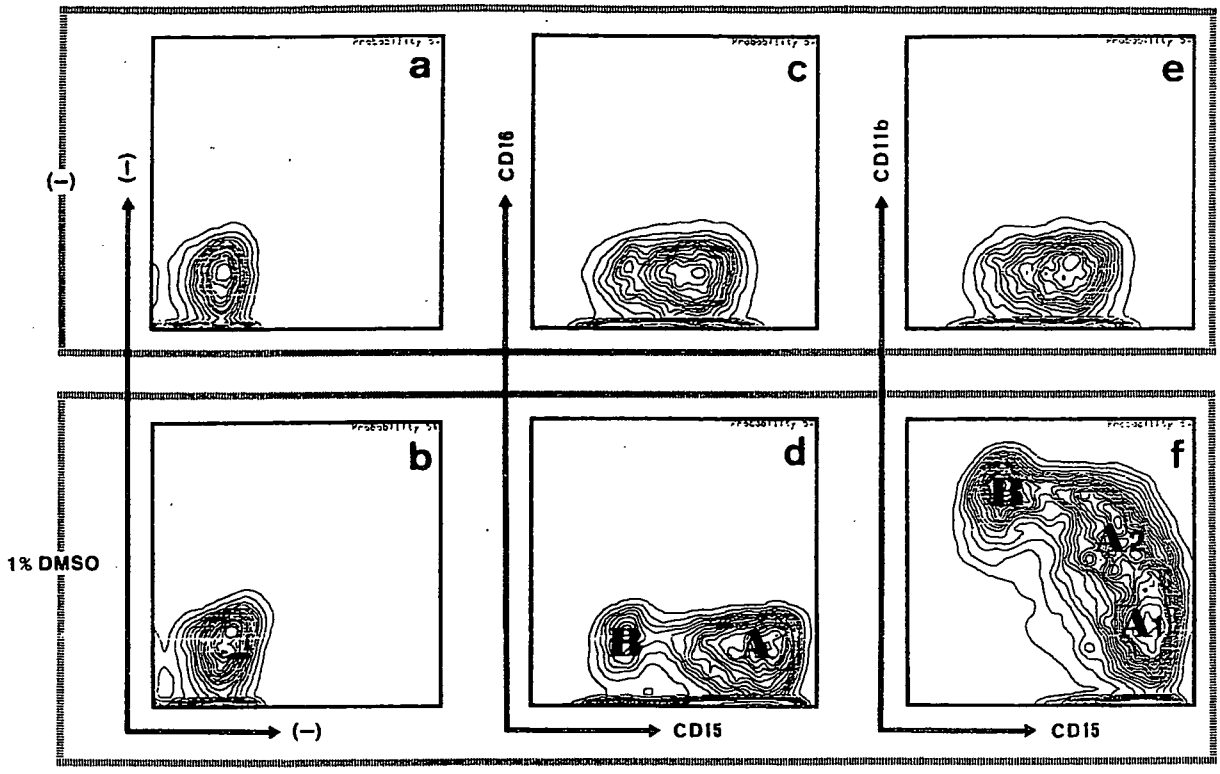

Fig. 1. Two-color FACS analysis of HL60 treated with (b, d, f) or without (a, c, e) 1% DMSO. Two-color staining was performed as follows: a and b: unstained; c and d: CD15(MX–GA) vs CD16(MG38); e and f: CD15(MX–GA) vs CD11b(Mol).

there were two cases of mutilating disease (MUD), six of the more erosive subset (MES), three of the least erosive subset (LES), and two that could not be classified because of the short duration of the disease. The controls were 8 joints from 8 patients with OA, one man and 7 women aged 48–70 (mean 58). All patients were diagnosed and treated at Oaska University Hospital.

Samples

Heparinized bone marrow blood was aspirated from the tibial proximal epiphysis during knee joint surgery, and mononuclear cell (MNC) fractions were separated by Ficoll-Paque

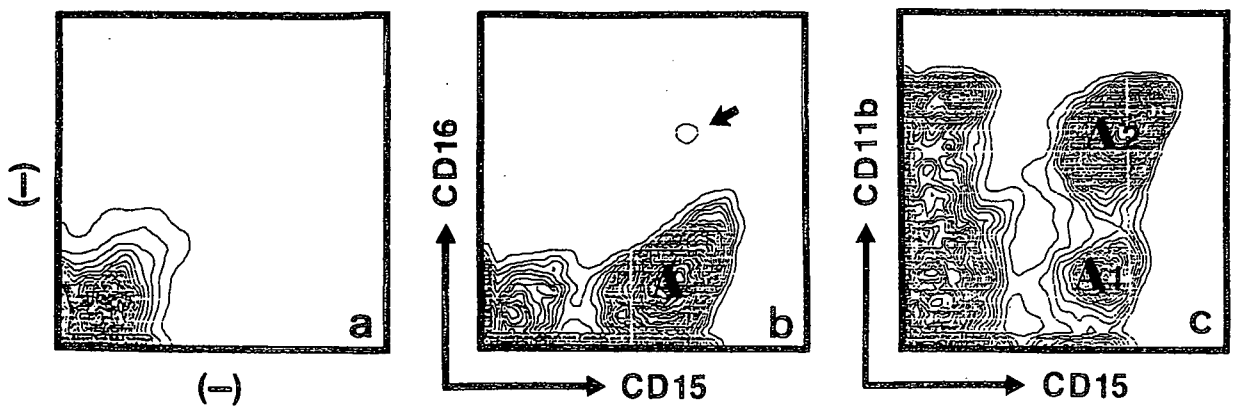

Fig. 2. Two-color FACS analysis of epiphyseal bone marrow MNCs from RA patients. a: unstained; b: CD15(MX–GA) vs CD16(MG38); c: CD15(MX–GA) vs CD11b(Mol).

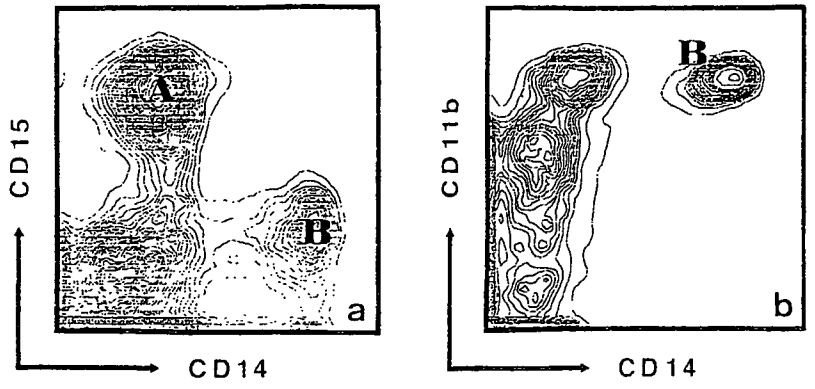

Fig. 3. Two-color FACS analysis of epiphyseal bone marrow MNCs from RA patients. a: CD14(Mo2) vs CD15(MX-GA); b: CD14(Mo2) vs CD11b(Mol).

(Pharmacia Fine Chemical, Sweden) discontinuous density gradient centrifugation (700 g, 20 min).

Cell line

HL60, a human myeloblastic leukemia cell line, was donated by Prof. Kishimoto (Institute for Molecular and Cellular Biology, Osaka University Medical School) and cultured in RPMI-1640 medium supplemented with 10% FCS, 2 mM of L-glutamine, 5×10^{-5} M of 2-mercaptoethanol, 100 U/ml of penicillin and 100 μg/ml of streptomycin. Some cells were cultured in the same medium, but supplemented with 1% DMSO during 7 days before FACS analysis.

Monoclonal antibodies

MX-GA antibody (CD15, clone HL5), which recognizes pan-myeloids, from myeloblasts to polymorphonuclear leukocytes (PMN)(7), and also reacts with HL60(8), was purchased from Kyowa Medex (Japan). MG38 antibody (CD16), which reacts with FCγ receptors on PMN, but not on natural killer (NK)(9), was purchased from Seikagaku-Kogyo (Japan). Mol antibody (CD11b), which reacts with relatively mature myeloids, from myelocytes to PMN, and also monocytes-macrophages(10), was purchased from Coulter Clone (USA). Mo2 antibody (CD14), which is a specific marker of monocytes-macrophages(10), was purchased from Coulter Clone. If fluorescence-isothiocyanate(FITC)- or biotin-labelled antibodies were not available, labelling was performed as previously described(11).

Two-color FACS analysis

Bone marrow MNCs were washed and suspended in a staining buffer (RPMI1640 deficient biotin, riboflavin and phenol red/2% FCS/10 mM HEPES/0.02% NaN_3) at a concentration of 10^6 cells/20 μl. Appropriately diluted FITC- or biotin-labelled antibodies were simultaneously added to the cell suspension in quantities of 10 μl each, and incubated for 20 min at 4°C. After washing with the staining buffer, 20 μl of Texas-Red avidin solution was added to the cell pellets which were then suspended. Incubated for 20 min at 4°C, propidium iodide (10 μg/ml) was also incubated during the last 5 min to label dead cells. Washed 3 times, cells were applied to a FACS440 (Becton Dickinson) equipped with a dual-laser system.

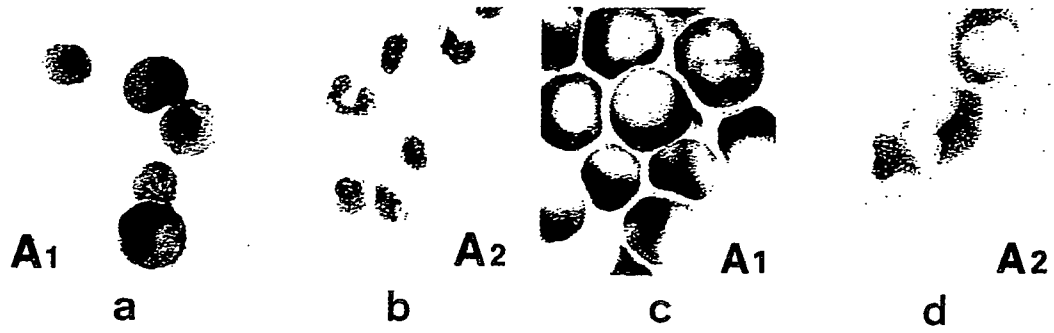

Fig. 4. Cytochemical staining of sorted cells. a and b: May-Grunwald; c and d: peroxidase staining. a and c: CD15-positive and CD11b-negative (A1) cells; b and d: CD15-positive and CD11b-positive (A2) cells.

Quantitative analysis

The gating in FACS was made on the plane of forward scatter and side scatter in each case, so as to remove the contaminated red blood cells. These could be clearly identified as small and no granular cells. The proportions of the number of each group of cells to that of whole MNCs were calculated by dividing the former by the latter.

Cytochemical staining

Sorted cells were attached to the glass slides with Cytospin (Shandon, England); some were stained with May-Grunwald and Giemsa solutions, and the others with peroxidase.

Classification of synovitis severity

The degree of synovitis was classified as follows, according to the findings at the surgical operations. (++): joint capsule was entirely covered with proliferated synovial cells; (+): about half of the capsular surface was covered with synovial proliferation; (±): synovitis was found only around the capsule-bone junction or bone-ligament junction; (−): there was no synovitis and the capsule was covered with fibrous tissue.

RESULTS

Two-color FACS analysis of HL60 cell line

The results for HL60 without chemical stimulation are shown in the upper row, and for HL60 treated with DMSO in the lower row, in Figure 1. HL60 cultured without DMSO reacted with CD15, but was not stained by CD16 nor CD11b (Figure 1 c and e). Cultured with DMSO, HL60 was not stained by CD16 either, but some cells (A) stained more brightly with CD15 (Figure 1 d). When stained with CD11b (Figure 1 f), these CD15-bright cells(A) were separated into two groups, CD11b-negative (A1) and -positive (A2).

Two-color FACS analysis of RA bone marrow MNC

One of the RA severe cases showed a FACS pattern similar to that of HL60 cultured with DMSO. There was a large number of cells (A) which reacted with CD15 (Figure 2 b), while the number of contaminated PMN was small (Figure 2 b, arrow). These CD15-positive cells

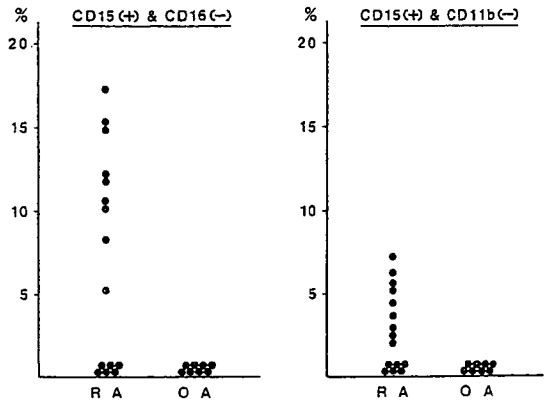

Fig. 5. Quantitative analysis of epiphyseal bone marrow myeloids from patients with RA or OA. The proportions of (A) or (A1) cells in MNCs are shown on the ordinate. (a): (A) cells = myeloids minus contaminated PMN; (b): (A1) cells = from myeloblasts to promyelocytes.

(A) could then be divided into CD11b-negative (A1) and CD11b-positive cells (A2) (Figure 2). Stained with CD14 and CD15, cells were clearly separated into three groups: CD15-positive cells (A), CD14-positive cells (B) and double-negative cells, but there existed no double-positive cells (Figure 3 a). All of the (B) cells reacted also with CD11b (Figure 3 b).

Cytochemical staining of sorted cells

The (A1) cells and (A2) cells seen in Figure 2 c were separately sorted by FACS. After being attached to glass slides, they were stained with May-Grunwald solution (Figure 4, a and b) or peroxidase (Figure 4, c and d). CD15-positive and CD11b-negative cells (A1) had a round nucleus and relatively large cytopasm (Figure 4 a). Their cytoplasmic granules were stained by peroxidase (Figure 4 c). CD15-positive and CD11b-positive cells (A2) showed a kidney-shaped nucleus (Figure 4 b), and their cytoplasmic large granules also stained with peroxidase. Consequently, (A1) cells showed the characteristics of myeloblasts-promyelocytes and (A2) cells those of myelocyte-metamyelocytes.

Quantitative analysis of myeloids in patients with RA or OA

Epiphyseal bone marrow MNCs from 15 joints with RA and 8 joints with OA were analyzed by FACS with results similar to those shown in Figure 2. The proportions of (A) or (A1) cells in epiphyseal bone marrow MNCs were calculated and are shown in Figure 5 on the ordinate. Nine of 15 joints with RA showed the existence of (A) cells (Myeloids minus contaminated PMN), with a range from 5.2% to 17.3% (mean: 11.8%) (Figure 5 a), while the others showed no myeloids (< 1%). The mean value for all RA joints was 7.1%. None of the patients with OA showed either (A) or (A1) cells. In RA patients, 9 joints with (A) Cells showed also (A1) cells (Myeloblasts-promyelocytes), with a range from 2.3% to 7.2% (mean 4.4%) (Figure 5 b). For all RA joints, the mean was 2.6%. Compared to (A) cells (Myeloids), the proportions of (B) cells (Macrophages) were more constant. In cases with RA (B) cells showed with a range from 8.7% to 16.3% (mean 12.7%), and OA showed with a range from 6.6% to 14.8% (mean 11.9%). There were no significant difference bitween RA and OA statistically.

Clinical features of RA joints

Profiles of patients with RA are listed in Table I, arranged according to the proportion of (A) cells. It was found that the group of joints with no (< 1%) (A) cells showed no synovitis, while none of the RA patients in subset LES had any (A) cells. Patients in subset MES who

Table I. Clinical features of RA joints and proportions of myeloids in bone marrow.

case	age	sex	disease period	disease subset	operat.	synovitis	(A): CD 15 (+) & CD 16 (−)	(A1): CD 15 (+) & CD 11b (−)
M.M	71	F	2 y	(ORA)	TKR(L)	(++)	17.3%	4.4%
M.Y	30	F	12 y	MUD	TKR(R)	(±)	15.3%	7.2%
K.K	57	F	13 y	MUD	TKR(L)	(−)	15.1%	5.6%
K.O	55	F	12 y	MES	TKR(R)	(+)	12.1%	6.2%
H.M	56	M	15 y	MES	TKR(R)	(+)	12.0%	5.2%
R.K	51	F	14 y	MES	TKR(R)	(+)	10.5%	3.6%
Y.D	47	F	7 y	(N.D.)	synovectomy	(++)	10.3%	2.6%
K.M	43	F	10 y	MES	TKR(R)	(+)	8.2%	2.4%
K.O	55	F	12 y	MES	TKR(L)	(+)	5.2%	2.3%
M.Y	34	F	12 y	MES	TKR(L)	(−)	<1.0%	<1.0%
S.Y	61	F	18 y	MES	TKR(R)	(−)	<1.0%	<1.0%
N.M	53	M	11 y	LES	TKR(R)	(±)	<1.0%	<1.0%
U.O	68	F	10 y	LES	TKR(R)	(−)	<1.0%	<1.0%
U.O	68	F	10 y	LES	TKR(L)	(−)	<1.0%	<1.0%
J.H	52	F	16 y	LES	TKR(L)	(−)	<1.0%	<1.0%

ORA: Old onset RA; N. D.: Not determined; TKR: Total knee replacement; MUD: Mutilating disease; MES; More erosive subset; LES: Least erosive subset.

had (A) cells showed (+) or (++) synovitis, but patients with MUD had many (A) cells although there was no evidence of synovitis.

DISCUSSION

Myeloid cells differentiate from bi-potential stem cells to PMN finally, and they have been traditionally characterized with cytochemical staining such as May-Grunwald, Giemsa and peroxidase. Later, some cytoplasmic markers for differentiation were found, such as lactoferrin(3) and inosine mono-phosphate(12), but they are not convenient for statistical or quantitative analysis. On the other hand, some cell surface antigens are known as differentiation markers of myeloids, namely, the C3bi and Fcγ receptors(13). The monoclonal antibodies for those receptors have been produced and are classified as CD11b and CD16, respectively. However, CD11b- or CD16- positive cells are not only myeloids, but also other lineage cells, so ti is necessary to purify the myeloids with cell-biological techniques or on the image of a FACS monitor. For the latter purpose, some monoclonal antibodies belonging to CD15 are useful, that is, they recognize only myeloid lineage cells, from myeloblasts to PMN. Double staining with CD15 monoclonal and CD11b or CD16 monoclonal, showed the differentiation stages of myeloids clearly, both in HL60 cell lines treated with DMSO and human bone marrow cells. Because of the simple staining method and quantitative analysis, this method could by useful for identifying the existence of immature myeloids.

We previously reported the elevated titers of myeloid growth activity in epiphyseal bone marrow adjacent to RA joints(2), and that this could be an important factor for abnormal myelopoiesis. It remains however unclear whether relatively mature myeloids invade in this site and proliferate or immature myeloids (or stem cells) differentiate and proliferate at this site. The results of the present study show a considerable number of immature myeloids besides relative mature cells, so that the latter hypothesis should be considered more likely.

The existence of myeloids in epiphyseal bone marrow in RA, is closely related to the clinical features of RA. Furthermore, disease subsets in RA and the degree of synovitis seem

to be important factors for this phenomenon. As for MES, synovial proliferation and the existence of myeloids are well correlated, so they may have a close pathological relationship. On the other hand, in the MUD subset, many myeloids exist in epiphyseal bone marrow without being accompanied by synovitis, so it is possible that myeloids appear independently of synovial lesions in this disease subset.

The mechanism of joint destruction in MUD seems to be different from that of the other types, where, the bone destruction begins as erosion at the capsule-bone junction. The destruction in MUD is so fast that it looks like a collapse of the bone structure. In view of these findings, the epiphyseal bone marrow in MUD could be the site of a severe reaction followed by osteoporosis and myelopoiesis, although these two may not directly correlate.

The functional abnormality of myeloids accumulating in epiphyseal bone marrow adjacent to joints with RA, is not clearly understood yet. However, PMN (the final differentiation stage of myeloids) in such lesions, are functionally different from those in other lesions in RA(14), and this function is most markedly shown in MUD cases. More detailed studies are needed to determine whether myeloids in such lessions also have an abnormal function as PMN do, and to understand the relation between myeloids and joint destruction in RA.

REFERENCES

1. Ochi T, Hakomori S, Adachi M, et al. The presence of a myeloid cell population showing strong reactivity with monoclonal antibody directed to difucosyl type 2 chain in epiphyseal bone marrow adjacent to joints affected with rheumatoid arthritis (RA) and its absence in the corresponding normal and non-RA bone marrow. J Rheumatol 1989; 15: 1609–15.
2. Owaki H, Ochi T, Yamasaki K, et al. Elevated activity of myeloid growth factor in bone marrow adjacent to joints affected by rheumatoid arthritis. J Rheumatol 1989; 16: 572–7.
3. Tado TA, Wei X, Benz EJ. Isolation of lactoferrin cDNA from a human myeloid library and expression of mRNA during normal and leukemic myelopoiesis. Blood 1987; 70: 989–93.
4. Collins SJ, Ruscetti FW, Gallagher RE, Gallo RC. Terminal differentiation of human promyelocytic leukemia cells induced by dimethyl sulfoxide and other polar compounds, Proc Natl Acad Sci USA 1987; 75: 2458–62.
5. Arnett FC, Edworthy SM, Bloch DA, et al. The American Rheumatism Association 1987 revised criteria for the classification of rheumatoid arthritis. Arthritis Rheum 1988; 31: 315–24.
6. Ochi T, Iwase R, Yonemasu K, et al. Natural course of joint destruction and fluctuation of serum Clq levels in patients with rheumatoid arthritis. Arthritis Rheum 1988; 31: 37–43.
7. Hamasima N, Uede R, Takahashi T. Characterization of three monoclonal antibodies that reach with high-molecular mass glycopeptides isolated from F9 mouse teratocarcinoma cells. Differentiation 1986; 31: 174–82.
8. Namikawa R, Ogata S, Uede R, et al. Serological analysis of cell surface antigens of HL-60 cells before and after treatment with a phorbor ester tumor promorter. Leuk Res 1983; 7: 375–87.
9. Tetteroo PAT. Van Der Schoot CE, Visser FJ, Bos MJE, Von Dem Borne AEGKR. Three different types of Fcγ Rlow of neutrophils, Fcγ Rlow of K/NK lymphocytes, and Fcγ RII. In: McMichael AJ eds. Leukocyte Typing III: White Cell Differentiation Antigens. Oxford/New York/Tokyo: Oxford University Press, 1987: 702–6.
10. Hogg N, Horton MA. Myeloid antigens: new and previously defined clusters. In: McMichael AJ eds. Leukocyte Typing III: Withe Cell Differentiation Antigens. Oxford/New York/Tokyo: Oxford University Press, 1987: 576–663.
11. Goding JW. Conjugation of antibodies with fluorochrome: modification of the standard methods. J Immunol Methods 1976; 13: 215–26.
12. Knight RD, Mangum J, Lucas DL, Cooney DA, Khan EC, Wright DG. Inosine monophosphate dehydrogenase and myeloid cell maturation. Blood 1987; 69: 634–9.
13. Glasser L, Fiederlein RL. Functional differentiation of normal human neutrophils. Blood 1987; 69: 937–44.
14. Wakitani S, Sakamuro D, Ochi T, Owaki H, Fujimoto M, Ono K. Polymorphonuclear cell factor found in patients with rheumatoid arthritis. Biomedical Research 1988; 9: 395–9.

Received 6 June 1990
Received revised 27 September 1990

Published in final edited form as:
Matrix Biol. 2007 March ; 26(2): 96–105.

OSTEOPONTIN PROMOTES PATHOLOGIC MINERALIZATION IN ARTICULAR CARTILAGE

Ann K. Rosenthal, MD, Claudia M. Gohr, BS, Miwa Uzuki, MD, PhD, and Ikuko Masuda, MD, PhD
From: The Division of Rheumatology, Department of Medicine, Medical College of Wisconsin and the Zablocki VA Medical Center, Milwaukee, WI

Abstract

Calcium pyrophosphate dihydrate (CPPD) crystals are commonly found in osteoarthritic joint tissues, where they predict severe disease. Unlike other types of calcium phosphate crystals, CPPD crystals form almost exclusively in the pericellular matrix of damaged articular cartilage, suggesting a key role for the extracellular matrix milieu in their development. Osteopontin is a matricellular protein found in increased quantities in the pericellular matrix of osteoarthritic cartilage. Osteopontin modulates the formation of calcium-containing crystals in many settings. We show here that osteopontin stimulates ATP-induced CPPD crystal formation by chondrocytes *in vitro*. This effect is augmented by osteopontin's incorporation into extracellular matrix by transglutaminase enzymes, is only modestly affected by its phosphorylation state, and is inhibited by integrin blockers. Surprisingly, osteopontin stimulates transglutaminase activity in cultured chondrocytes in a dose responsive manner. As elevated levels of transglutaminase activity promote extracellular matrix changes that permit CPPD crystal formation, this is one possible mechanism of action. We demonstrate the presence of osteopontin in the pericellular matrix of chondrocytes adjacent to CPPD deposits and near active transglutaminases. Thus, osteopontin may play an important role in facilitating CPPD crystal formation in articular cartilage.

Keywords

Osteopontin; Calcium pyrophosphate dihydrate; Transglutaminase; Osteoarthritis

Pathologic matrix mineralization is a common occurrence in joints affected by late stage osteoarthritis. Of synovial fluids sampled at the time of knee replacement, for example, 60% contain pathologic calcium-containing crystals (Derfus et al. 2002). Both calcium pyrophosphate dihydrate (CPPD) and hydroxyapatite-like basic calcium phosphate (BCP) crystals occur in osteoarthritic joints. Although the role that calcium-containing crystals play in osteoarthritis is not fully understood, there is ample evidence to suggest that these crystals are active participants in joint damage. *In vitro*, calcium-containing crystals induce the release of catabolic cytokines and proteases from synovial cells and chondrocytes (Cheung 2001). Clinically, their presence predicts increased severity of joint damage and more rapid progression of joint destruction (Ledingham et al. 1993; Nalbant et al. 2003).

Corresponding Author: Ann K. Rosenthal, MD Rheumatology Section/ cc-111W Zablocki VA Medical Center 5000 W. National Ave. Milwaukee, WI 53295-1000 TEL: 414-384-2000, ext 42760 FAX: 414-383-8010 Email:ann.rosenthal@med.va.gov.

While BCP crystals are similar in structure and composition to mineral found in normal bone and at many sites of pathologic mineralization, CPPD crystals are relatively unique to hyaline and fibro-cartilages (McCarty et al. 1966). Indeed, when found in other tissues, CPPD crystals are often seen within sites of chondroid metaplasia (Beutler et al. 1993). The smallest and presumably the earliest CPPD crystals occur in the pericellular matrix surrounding articular chondrocytes (McCarty 1972). This narrow tissue distribution suggests that the unique milieu of cartilage extracellular matrix may be necessary for CPPD crystal formation.

CPPD crystals are formed when several conditions are met. High local concentrations of extracellular inorganic pyrophosphate, the anionic component of the crystal, are clearly necessary for CPPD crystal formation (Ryan et al. 2003). Sufficient levels of extracellular calcium must also be available. Lastly, a solid matrix is crucial for CPPD crystal formation, as conditions for crystallization in solution require supra-physiologic concentrations of ions and extremes of pH and temperature (Mandel et al. 1984).

While considerable attention has been paid to other modulators of CPPD crystal formation, such as pyrophosphate production, relatively little is known about the role of extracellular matrix in this process. CPPD crystals are rarely found in areas of normal articular cartilage matrix (Bjelle 1981), suggesting that alterations in matrix composition and/or ion composition are necessary for crystallization. Ishikawa et al. demonstrated fragmented type II collagen fibers, loss of large proteoglycans, and increased levels of calcium-binding matricellular proteins in cartilage affected by CPPD crystal deposits (Ishikawa et al. 1989; Masuda et al. 1991). Matrix-modifying enzymes known as transglutaminases have also been implicated in CPPD crystal formation (Heinkel et al. 2004). Inhibition of transglutaminase activity in chondrocytes abrogates CPPD crystal formation in vitro (Heinkel et al. 2004). Transglutaminase protein levels and enzymes activities are increased in the extracellular matrix of osteoarthritic articular cartilage (Johnson et al. 2001; Summey et al. 2002), the setting in which CPPD crystals are most common. Although the mechanism through with they promote CPPD crystal formation is unclear, transglutaminases anchor their substrates to matrix and likely alter the composition, structure, and function of affected matrices (Lorand et al. 2003).

Although extracellular matrix composition plays an important role in CPPD crystal formation and growth, the cartilage matrix components that modulate mineralization remain largely unidentified. Osteopontin is a 44-66 kDa calcium-binding matricellular protein present in articular cartilage (Lorand et al 2003; Giachelli et al. 2005) . We became interested in osteopontin as a potential modulator of CPPD crystal formation in articular cartilage for the following reasons: 1). Osteopontin is present at sites of both normal and pathologic matrix mineralization and is a well-characterized modulator of mineralization (Giachelli et al. 2005). 2). Osteopontin has a pericellular distribution in cartilage (Parikh et al. 2003), and is found in increased concentrations in osteoarthritic cartilage (Pullig et al. 2000). 3). Osteopontin is an important substrate of the transglutaminase enzymes in mineralizing tissues (Beninati et al. 1994; Kaartinen et al. 1999).

Osteopontin is almost ubiquitous at sites of both normal and pathologic mineralization. However, its role in mineral formation remains poorly understood and somewhat controversial. Osteopontin typically inhibits growth of calcium-containing crystals in models of bone mineralization and nephrolithiasis (Beshensky et al. 2001; Steitz et al. 2002). Similar effects have recently been demonstrated in a gel-based model of hydroxyapatite crystal formation (Gericke et al. 2005). Fewer studies support a stimulatory role for osteopontin in mineralization (Wozniak et al. 2000). It is likely that high levels of soluble osteopontin act directly on crystal nucleation or growth. Highly anionic osteopontin may limit the size of calcium-containing crystals by binding to existing crystals and preventing further growth. Alternatively, osteopontin may act through other intermediaries. Osteopontin is present in almost every tissue,

and is known to act as a signaling protein and cytokine, as well as a regulator of mineralization (Denhardt et al. 2001). Osteopontin interacts with the αvβ3 integrin (Wozniak et al. 2000) and mediates cell adhesion and differentiation, which in turn could alter cell phenotype and matrix mineralization. In osteoblasts, osteopontin production is coordinately regulated with elaboration of inorganic pyrophosphate, a potent inhibitor of hydroxyapatite crystal formation (Johnson et al. 2003; Harmey et al. 2004). Thus, osteopontin may indirectly affect mineralization by altering levels of other crystal-regulating substances.

A commonly invoked explanation for the varied effects of osteopontin both *in vivo* and *in vitro* entails variations in osteopontin's extensive post-translational modifications. Osteopontin contains sites for phosphorylation, glycosylation, transglutamination, and thrombin cleavage. Transglutaminase covalently binds osteopontin to fibronectin, to itself, and to other matrix constituents (Kaartinen et al. 1999). Functional alterations due to these post-translational modifications are well-described. Osteopontin's phosphorylation state and whether it is matrix-bound or soluble may be particularly important determinants in its effects in mineralization models (Jono et al. 2000).

The present studies were designed to determine whether osteopontin modulated CPPD crystal formation in articular cartilage. We first determined the effects of osteopontin in a well-characterized model of CPPD crystal formation by chondrocytes (Ryan et al. 1992), and were surprised to find a stimulatory effect. We then determined whether post-translational modifications altered osteopontin's ability to promote CPPD crystal formation, and explored potential mechanisms of this effect. Lastly, we confirmed the presence of osteopontin in the matrix around CPPD crystal deposits in diseased human cartilage.

METHODS

Materials

Purified milk and recombinant bovine osteopontin were from R& D Systems (Minneapolis, MN). The integrin-binding antagonist GRGDS and a control peptide GRGES were from (NeoMPS, Strasbourg, France).

Porcine chondrocyte cultures

Porcine chondrocytes were isolated from hyaline cartilage removed from the patellar and femoral surfaces of 3-5 year old pigs (Johnsonville Foods, Inc., Watertown, WI) by sequential enzymatic digestion (Rosenthal et al. 1991). Chondrocytes were plated at 4×10^5 cells/cm^2 in Dulbecco's Modified Eagle's Medium (DMEM, Mediatech, Herndon, VA) with 10 % fetal calf serum in 24-well tissue culture plates. Twenty-four hours before beginning an experiment, media were replaced with serum-free media. Experiments were performed in 50 mM HEPES-buffered DMEM with 0.35 mg/ml bovine serum albumin (experimental media) within 5 days of plating. These culture conditions maintain the highly differentiated chondrocyte phenotype in short term cultures (Mitchell et al. 1992).

ATP-induced calcification (Ryan, Kurup et al. 1992)

In this model, the precipitation of ^{45}Ca by chondrocyte monolayers in the presence of 1 mM ATP correlates with the formation of CPPD crystals, as characterized by morphology, susceptibility to digestion with pyrophosphatase and inorganic pyrophosphate content. Non-specific ^{45}Ca binding is determined by running simultaneous controls with no added ATP. In some experiments, an additional control group with 1mM β-glycerophosphate was added to control for non-specific effects of phosphate. Chondrocytes were cultured in experimental media trace- labeled with 1 μCi/ml ^{45}Ca with or without 1 mM ATP or β-glycerophosphate, and with or without various concentrations of osteopontin. After 48 hours, media were

removed, and the cell layer was exhaustively washed with cold Hank's Balanced Salt Solution. The cell layer was treated with 0.1 N NaOH for one hour at 37°C, and radioactivity in the cell layer was quantified by liquid scintigraphy. Values were corrected for protein levels in the cell layers using the Lowry assay.

Post-translational modifications of osteopontin

De-phosphorylation of osteopontin—Purified bovine milk osteopontin was de-phosphorylated using alkaline phosphatase attached to agarose beads (Sigma Chemical Co., St Louis, MO) according to the method of Jono et al. (Jono et al. 2000). This allows for removal of the alkaline phosphatase enzyme prior to exposure to cells, and is estimated to remove 85% of phosphate residues (Goldberg et al. 1995). Protein levels were determined after alkaline phosphatase treatment, so as to correct for any protein lost during processing. To ensure that phosphate was removed from osteopontin during this procedure, inorganic phosphate levels were measured in the osteopontin solution before and after exposure to alkaline phosphate using the QuantiChrom ™ assay (Bioassay Systems, Hayward, CA). During 2 hours of exposure to alkaline phosphatase beads, inorganic phosphate levels in the osteopontin solution increased and plateaued. (Data not shown). To further demonstrate quantitative phosphate removal, we used a stain for phosphorylated proteins (GelCode Phosphoprotein Stain Reagent Set, Pierce, Rockford, IL). Identical quantities of various preparations of osteopontin were loaded onto an SDS gel, and stained according to the manufacturer's directions.

Thrombin cleavage—To determine the effect of thrombin treatment on osteopontin, osteopontin was treated with thrombin attached to agarose beads (Sigma Chemical Co.) for 15 minutes at 37° C. Beads were removed and protein levels were measured to correct for protein lost during processing. SDS-PAGE was performed to confirm quantitative cleavage.

Transglutaminase inhibition—Transglutaminase activity in chondrocytes was inhibited with 125μM cystamine or 1 mM monodansylcadaverine. We have shown previously that these concentrations of inhibitors reduce transglutaminase activity in chondrocytes by 50-90% without significant toxicity (Heinkel et al. 2004).

Osteopontin and aggrecan ELISAs

Osteopontin levels were measured in the cell layer using a commercial ELISA (Assay Designs, Ann Arbor, MI). Levels of aggrecan were measured in an identical manner using an ELISA kit (Biosource, Nivelles, Belgium). Media were removed from chondrocyte cultures. After washing, the cell layer was scraped into the assay buffer supplied with each kit. Levels of specific proteins were corrected for total cell layer protein as measured by the Lowry assay.

Determination of pyrophosphate levels

Inorganic pyrophosphate levels were measured in chondrocyte conditioned media as previously described (Rosenthal et al. 1991). This method is based on the enzymatic conversion of ^{14}C UDPG to ^{14}C glucose-1-phosphate and uridine triphosphate in the presence of pyrophosphate. Differential charcoal absorption of ^{14}C UDPG before and after enzymatic conversion directly reflects pyrophosphate levels.

Identification of transglutaminase-specific crosslinks in osteopontin (Ishikawa et al. 1989; Masuda et al. 1991)

We isolated osteopontin from a guanidine extract of porcine articular cartilage using an immunoaffinity column (ImmunoPure Plus IgG Orientation Kit, Pierce, Rockford, IL) with a polyclonal osteopontin antibody (Chemicon). After exhaustive digestion, transglutaminase-specific ε–(γ glutamyl) lysine crosslinks were quantified in osteopontin by HPLC as previously

described (Heinkel et al. 2004). The purity of the immunopurified protein was determined by running the sample on an SDS-PAGE gel, followed by Western blotting.

Transglutaminase activity and enzyme levels

Transglutaminase activity was measured using a standard radiometric assay based on incorporation of ^{3}H putrescine into casein as previously described (Rosenthal et al. 1997). Factor XIIIA and type II transglutaminase protein levels were estimated by Western blotting (Rosenthal et al. 2004).

Chondrocyte viability

Chondrocyte viability under various experimental conditions described was measured with a standard assay based on leakage of LDH with cell injury (Genotech, St. Louis, MO).

Human cartilage samples

Preserved, de-identified, paraffin-embedded human knee cartilage samples were obtained from patients with CPPD deposition disease. These tissue specimens were obtained from hospitals affiliated with Iwate Medical University Hospital, Morioka, Tohoku University Hospital, Sendai or Kumamoto University Hospital, Kumamoto, Japan from 1995 to 2003. Informed consent was obtained from each patient. The study has been carried out in accordance with the Declaration of Helsinki (1989) of the World Medical Association, and has been approved by the IRBs of the hospitals involved.

Immunohistochemistry

After de-paraffinization, sections for osteopontin immunostaining were pretreated at 37° C for 10 minutes with 1mg/ml of trypsin diluted in 9 mM calcium chloride at pH 7.4. Sections for N ε-(γ-glutamyl) lysine isopeptide immunostaining were pretreated at 37° C for 30 minutes with 40 mU/ml of chondroitinase ABC (Seigagaku, Rockville, MD) diluted in 30mM sodium acetate and 10mM Tris-HCl at pH 7.4. Washed sections were treated with 0.3% (V/V) hydrogen peroxide for 30 minutes at room temperature and with 10% (V/V) normal goat serum for 40 minutes at room temperature. Sections were incubated with anti- N ε-(γ-glutamyl) lysine isopeptide mouse monoclonal antibody (1:100, CovaLab, Lyon, France) or rabbit anti-human osteopontin (1:1500, Chemicon, Temecula, CA) overnight at 4°C. After washing, sections were treated with the appropriate biotinylated anti-IgG for 30 minutes at room temperature. Antibody staining was detected with avidin-biotin-antiperoxidase complex (ABC kit; Vector Laboratories Inc., Burlingame, CA). Antigenic sites were demonstrated by reacting the sections with a 3,3′ diaminobenzidine tetrahydrochloride (DAB: Sigma Chemical Co., USA) for 7 min. Sections were counterstained with methyl green, dehydrated in ethanol, cleared in xylene and mounted. Non-immune mouse (for N ε-(γ-glutamyl) lysine isopeptide) or rabbit (for osteopontin) IgG was used in place of the primary antibody in the negative controls.

Statistics

All experiments were repeated at least 3 times. A student's T test was used to determine statistical significance between groups.

RESULTS

The effect of osteopontin on CPPD crystal formation by articular chondrocytes

To explore the role of osteopontin in CPPD crystal formation, we employed a well characterized model based on the ATP-dependent accumulation of calcium in articular chondrocyte cultures. In this model, ^{45}Ca precipitated in the cell layer in the presence of ATP forms CPPD crystals, as previously proven by chemical analysis, morphologic observations,

and susceptibility to digestion by pyrophosphatase (Ryan et al. 1992). A significant advantage of this model is that simple calcium binding or calcium uptake by chondrocytes is controlled for by measuring ^{45}Ca in the absence of ATP. As shown in Figure 1, the addition of 1 μg/ml recombinant osteopontin to chondrocytes increased quantities of ^{45}Ca in the cell layer by 2.4 ± 0.04 fold in the presence of ATP compared to control values without osteopontin (n = 25, $p<0.01$). Osteopontin had no effect on ^{45}Ca accumulation in the absence of ATP, or in the presence of 1 mM β glycerophosphate. These results suggest that this effect is not a non-specific effect related to osteopontin's calcium binding capacity, nor is it an effect from added phosphate. As shown in Figure 2, recombinant osteopontin increased ATP-induced ^{45}Ca accumulation at doses as low as 0.1 μg/ml with maximal activity at 1 μg/ml. Concentrations below 0.1 μg/ml or above 10 μg/ml did not statistically significantly stimulate CPPD crystal formation. Osteopontin had no effect on the viability of chondrocytes at any of the concentrations tested. (Data not shown). The morphology of crystals formed in the presence of osteopontin and ATP is identical to that seen with ATP alone under polarizing light microscopy and demonstrates the characteristic positive birefringence of CPPD crystals (Figure 3).

The effect of de-phosphorylation and thrombin cleavage on osteopontin's ability to stimulate CPPD crystal formation

The phosphorylation state of osteopontin may have dramatic effects of on its behavior in mineralization models. For example, several studies have shown that highly phosphorylated osteopontin had opposite effects on mineral formation compared to un-phosphorylated forms (Jono et al. 2000; Gericke et al. 2005). We examined the effects of highly phosphorylated milk osteopontin on CPPD crystal formation. As seen in Figure 4, the dose response curve seen with milk osteopontin is very similar to that seen with the less phosphorylated recombinant protein. To confirm these results, we compared the effects of phosphorylated and de-phosphorylated milk osteopontin on CPPD crystal formation. After de-phosphorylation of milk osteopontin with alkaline phosphatase-coated beads, osteopontin retained its ability to stimulate CPPD crystal formation ($p<.05$), with a small decrease in efficacy ($p<.05$) (Figure 5). Using a stain for phosphorylated proteins (Figure 6), we confirmed a significant removal of phosphate moieties from milk osteopontin using alkaline phosphatase-coated beads. This stain also demonstrated fewer phosphates per milligram protein in recombinant osteopontin compared to milk osteopontin (Figure 6). Taken together, these results suggest that osteopontin's ability to stimulate CPPD crystal formation is not fully dependent on its phosphorylation state.

Thrombin cleavage may also alter the behavior of osteopontin (Yamamoto et al. 2003). The thrombin cleavage site is near the integrin binding site in the osteopontin molecule, yet thrombin cleavage stimulates integrin binding in some cell types (Yokosaki et al. 2005). Exposure of milk osteopontin to thrombin-coated beads, reduced osteopontin's effect on CPPD crystal formation so as to quantitatively eliminate its stimulatory effect ($p=0.25$) (Figure 5). Quantitative cleavage of osteopontin by thrombin is confirmed in Figure 6. These data suggest that an intact osteopontin molecule is necessary for an optimal effect. Neither de-phosphorylation nor thrombin-cleavage altered the effect of osteopontin on ^{45}Ca precipitation by chondrocytes in the absence of ATP. (Data not shown).

The effect of transglutaminase-inhibitors on osteopontin levels in extracellular matrix

To confirm that osteopontin is a substrate for endogenous transglutaminases in articular chondrocytes, we determined the effects of transglutaminase inhibitors on osteopontin levels in chondrocyte cell layers. Transglutaminase inhibitors reduced osteopontin levels in chondrocyte cell layers (Figure 7). Cystamine decreased osteopontin levels to 46 ± 3% of control values, while monodansylcadaverine decreased osteopontin levels to 67 ± 2 % of control values ($n=6$, $p< 0.05$). In contrast, levels of aggrecan, a matrix protein not known to

be a transglutaminase substrate, were unchanged by the addition of transglutaminase inhibitors. These data confirm transglutaminase-dependent extracellular matrix incorporation of osteopontin. Levels of osteopontin and aggrecan in the media were unchanged after cystamine exposure compared to control values. Aggrecan and osteopontin levels in the media significantly decreased in the presence of monodansylcadaverine in the setting of a decrease in total protein synthesis frequently caused by monodansylcadaverine (Data not shown).

Transglutaminase crosslinks in osteopontin from articular cartilage

Further evidence that osteopontin is a transglutaminase substrate in articular cartilage is evidenced by the direct measurement of the transglutaminase-specific dipeptide ε–(γ glutamyl) lysine in osteopontin isolated from porcine cartilage. Osteopontin was isolated from porcine cartilage using immunoprecipation. This resulted in two bands on SDS-PAGE gel. Both were immunoreactive with anti-osteopontin. (Data not shown.) Levels of crosslink were 202 ± 43 nmoles glutamyl-lysine crosslink /mg protein. This level is similar to that of osteonectin, also a known transglutaminase substrate in cartilage.

The stimulatory effect of osteopontin on CPPD crystal formation requires active transglutaminases

We next explored the hypothesis that transglutaminase-mediated binding of osteopontin to chondrocyte matrix affects its ability to promote CPPD crystal formation. We incubated chondrocytes with millk osteopontin in the presence of transglutaminase inhibitors and measured CPPD crystal formation. As shown in Figure 8, the transglutaminase inhibitors, cystamine and monodansylcadaverine, suppressed the stimulatory effects of osteopontin on CPPD crystal formation. Compared to osteopontin alone, ^{45}Ca levels fell significantly with osteopontin and cystamine, and osteopontin and monodansylcadaverine, in the presence of ATP. Indeed, in the absence of active transglutaminases, osteopontin failed to stimulate CPPD crystal formation. Confirming our previous findings, transglutaminase inhibition alone decreased levels of ATP-induced ^{45}Ca precipitation in chondrocytes (Heinkel et al. 2004). No effects were seen in the absence of ATP. These data suggest that transglutaminase-mediated incorporation of osteopontin into chondrocyte matrix promotes its stimulatory effects on CPPD crystal formation.

The effect of osteopontin on pyrophosphate and transglutaminase levels

The mechanisms through which osteopontin participates in crystal formation are unclear. Osteopontin, particularly at high concentrations, directly inhibits hydroxyapatite crystal growth by coating existing crystals with highly anionic protein (Goldberg et al. 1995; Gericke et al. 2005). Lower concentrations of osteopontin may affect mineralization through other mechanisms. Pyrophosphate is an antagonist of hydroxyapatite crystal growth, but is a participant in CPPD crystal formation. It is possible that osteopontin indirectly affects CPPD crystal formation by stimulating pyrophosphate production. Alternatively, osteopontin could increase the expression or activity of the transglutaminase enzymes, and thus could contribute to CPPD crystal formation through this mechanism. To address the mechanism of the effect of osteopontin on CPPD crystal formation, we asked whether osteopontin could increase pyrophosphate elaboration or transglutaminase activity levels in cultured chondrocytes. As shown in Table 1, milk osteopontin did not significantly affect pyrophosphate levels in chondrocyte cultures. In contrast, osteopontin did increase transglutaminase activity levels in a dose-responsive manner (Figure 9). This action would further increase the matrix incorporation of osteopontin as well as other mineralization-promoting matrix components.

Interestingly, maximally stimulatory doses of osteopontin had little effect on protein levels for the transglutaminases present in articular chondrocytes. One μg/ml of milk osteopontin did not increase protein levels of either type II transglutaminase or factor XIIIA as measured by

Western blotting. (Data not shown). Thus, it is likely that osteopontin increases activity of these enzymes without altering their levels. Both enzymes are often regulated at post-translational levels (Lorand et al. 2003), and further work will be necessary to investigate the mechanism of this effect.

The role of αvβ3 integrin in osteopontin's effects

Wozniak et al. elegantly demonstrated that mineralization in bone cell cultures occurs in plaques containing large macromolecular complexes of osteopontin crosslinked by transglutaminases. They showed this early pericellular mineralization process was dependent on the αvβ3 integrin (Wozniak et al. 2000). To determine if the effects of osteopontin in our system were integrin-dependent, we blocked integrin binding with an antagonist peptide. As shown in Figure 10, the active antagonist peptide GRGDS suppressed the effect of milk osteopontin on CPPD crystal formation to about 50% of control values. The control peptide had less of a consistent effect. This experiment was repeated with multiple doses of peptides (Data not shown). While the GRGES peptide had no statistically significant effect on osteopontin-induced CPPD crystal formation at doses of 5-40 μM (142% of osteopontin alone, $p = .06$), the GRGDS peptide significantly reduced osteopontin-induced CPPD crystal formation at all doses tested (57% of osteopontin alone, $p < .001$) Thus, it appears that osteopontin's effect on CPPD crystal formation may at least be partially mediated through integrin binding.

Osteopontin and transglutaminase activity in human cartilage affected by CPPD crystal deposition

If osteopontin participates in CPPD crystal formation, it should be present in the extracellular matrix of articular cartilage from patients with CPPD deposition disease. Immunohistochemistry with osteopontin antibody demonstrated the presence of osteopontin protein in the pericellular matrix near CPPD crystal deposits (Figure 11A), while a negative control performed with non-immune serum showed little staining (Figure 11B). This pericellular distribution correlates well with the distribution of the smallest and presumably the earliest CPPD crystals. Obviously, no conclusions can be made from these studies as to the chronology of the appearance of the crystals in relation to osteopontin. We also examined the same human cartilage samples for evidence of *in vivo* transglutaminase activity by staining with an antibody that recognizes the ε–(γ glutamyl) lysine bond formed by transglutaminases. The pericellular pattern of distribution of transglutaminase-specific crosslinks was similar to that of osteopontin (Figure 11C), further supporting a role for transglutaminases in mediating incorporation of osteopontin into cartilage matrix. Again, no staining was seen when the primary antibody was replaced with non-immune serum (Figure 11D).

DISCUSSION

We show here that osteopontin is present in the extracellular matrix near CPPD crystal deposits in articular cartilage and that it stimulates CPPD crystal formation by articular chondrocytes *in vitro*. Our model of CPPD crystal formation is based on the formation of CPPD crystals by cultured chondrocytes in the presence of the ATP (Ryan et al. 1992). Crystals formed under these conditions have previously been proven to be CPPD crystals by polarizing light microscopy, pyrophosphate content, electron beam diffraction and dissolution with pyrophosphatase. Osteopontin had no effect on ^{45}Ca precipitation in the absence of ATP or in the presence of β-glycerophosphate. Taken together, we believe these data demonstrate that osteopontin specifically stimulates CPPD crystal formation, and that this effect is not due to a non-specific increase in calcium binding to the cell layer nor is it a response to exogenous phosphate. Thus, increased levels of osteopontin such as those that occur in osteoarthritic cartilage, could promote CPPD crystal formation.